

Article

Degradation of Ibuprofen by the Electro/Fe³⁺/Peroxydisulfate Process: Reactive Kinetics, Degradation Products and Mechanism

Na Qiu ¹, Chanchan Shen ^{1,*}, Yongxia Liu ¹, Xiuqing Li ², Guangyin Jia ¹, Jingping Qin ¹ and Xinglei Wang ¹

¹ College of City and Architecture Engineering, Zaozhuang University, Zaozhuang 277160, China; wendy65066@163.com (N.Q.); 3319901@sohu.com (Y.L.); yunyang2022@126.com (G.J.); qinjingping123@163.com (J.Q.); wangxinglei412@163.com (X.W.)

² Shandong Province Research Institute of Coal Geology Planning and Exploration, Jinan 250104, China; lixiuqingcp@126.com

* Correspondence: shenchan1208@126.com

Abstract: Ibuprofen (IBU), a nonsteroidal anti-inflammatory drug, is one of the most widely used and frequently detected pharmaceuticals and personal care products in water bodies. This study examined the IBU degradation in aquatic solutions via ferric ion activated peroxydisulfate (PDS) coupled with electro-oxidation (EC/Fe³⁺/PDS). The degradation mechanisms involved three synergistic reactions in the EC/Fe³⁺/PDS system, including: (1) the electro-oxidation; (2) SO₄^{•−} generated from the activation of PDS by ferrous ions formed via cathodic reduction; (3) SO₄^{•−} generated from the electron transfer reaction. The radical scavenging experiments indicated that SO₄^{•−} and •OH dominated the oxidation process. The effects of the applied current density, PDS concentration, Fe³⁺ dosage, initial IBU concentration and initial pH as well as inorganic anions and humic acid on the degradation efficiency, were studied, and the degradation process of IBU followed the pseudo-first-order kinetic model. About 99.37% of IBU was removed in 60 min ((Fe³⁺ concentration) = 2.0 mM, (PDS concentration) = 12 mM, (initial IBU concentration) = 30 mg/L, current density = 15 mA/cm², initial pH = 3). Finally, seven intermediate compounds were identified and probable IBU degradation pathways in the EC/Fe³⁺/PDS system were speculated.

Keywords: sulfate radicals; hydroxyl radicals; electro-oxidation; mechanism; degradation



Citation: Qiu, N.; Shen, C.; Liu, Y.; Li, X.; Jia, G.; Qin, J.; Wang, X. Degradation of Ibuprofen by the Electro/Fe³⁺/Peroxydisulfate Process: Reactive Kinetics, Degradation Products and Mechanism. *Catalysts* **2022**, *12*, 329. <https://doi.org/10.3390/catal12030329>

Academic Editor: Ioannis Konstantinou

Received: 29 January 2022

Accepted: 11 March 2022

Published: 13 March 2022

Publisher's Note: MDPI stays neutral with regard to jurisdictional claims in published maps and institutional affiliations.



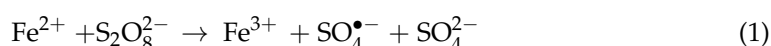
Copyright: © 2022 by the authors. Licensee MDPI, Basel, Switzerland. This article is an open access article distributed under the terms and conditions of the Creative Commons Attribution (CC BY) license (<https://creativecommons.org/licenses/by/4.0/>).

1. Introduction

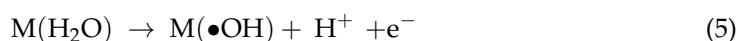
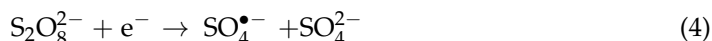
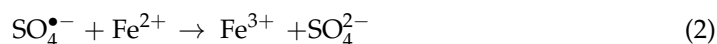
Ibuprofen (IBU), a non-steroidal anti-inflammatory drug, is extensively used to treat fever and pain, including muscle aches, tooth aches, headache pain and arthritis pain [1,2]. The annual global production of IBU was more than 30 kilotons due to its widespread utilization in aquaculture, domestic, hospitals and pharmaceutical industries [3]. IBU has been frequently found in municipal and hospital wastewater with concentrations of up to 83 µg/L [4]. Conventional wastewater treatment technologies (e.g., activated sludge, coagulation and filtration) are usually not effective to remove IBU, resulting in the relatively high concentration of IBU in wastewater treatment plants (WWTPs) effluents [5–7]. Constant discharge of IBU into the aquatic environment may pose threat to human health and affect the safety and balance of the aquatic ecosystem [8,9]. For instance, IBU could change the intestinal microbial composition of humans via long-term consumption [10] and the endocrine system could be altered by IBU, inducing compensated hypogonadism in men [11]. Moreover, apoptosis and a decrease in proliferating cells of humans might occur after exposure to 10–100 µmol/L of IBU [12]. As reported, IBU may pose acute toxicity to the reproduction of some aquatic organisms, for example, Japanese medaka and zebrafish [10,13]. Additionally, IBU could promote cyanobacteria and reduce the eukaryotic algae biomass, resulting in algal blooms in freshwaters [14]. IBU also had an adverse

impact on the reproduction and the survival of *Oryzias latipes* as well as the growth of algae *Synechocystis* sp. [15]. Therefore, the development of suitable technologies for removing the IBU efficiently from water is of great urgency.

Recently, advanced oxidation methods, involving the generation of hydroxyl radical ($\bullet\text{OH}$), sulfate radical ($\text{SO}_4^{\bullet-}$), were considered as effective technologies for the treatment of IBU [16–18]. Compared with $\bullet\text{OH}$ ($E_0 = 2.8$ V), $\text{SO}_4^{\bullet-}$ also exhibits strong oxidizing ability ($E_0 = 2.5$ – 3.1 V) [19–21]. Furthermore, $\text{SO}_4^{\bullet-}$ has longer lifetimes (1 μs for $\bullet\text{OH}$ vs. 30–40 μs for $\text{SO}_4^{\bullet-}$), higher selectivity, as well as a broad operative range of pH. Generally, $\text{SO}_4^{\bullet-}$ is produced by activating peroxydisulfate (PDS) or peroxymonosulfate (PMS) with transition metals, heat, UV, electrochemical and ultrasound. Parallel to other transition metals, Fe^{2+} has been commonly used for the activation of PDS (Equation (1)) since it is inexpensive, effective and environmentally friendly [22].



However, some drawbacks of the Fe^{2+} /PDS process hinder its application [23]. Firstly, Fe^{2+} could not be regenerated after transformation to Fe^{3+} , leading to a high Fe^{2+} dosage requirement to maintain the reaction. As a result, the process produces a larger amount of iron sludge [24]. Secondly, excessive Fe^{2+} would act as a scavenger for $\text{SO}_4^{\bullet-}$ (Equation (2)). Finally, Fe^{2+} is readily converted to Fe^{3+} in the existence of oxygen in the air. The above drawbacks could be solved by the coupling of the Fe^{3+} /PDS system with the electrochemical system (EC/ Fe^{3+} /PDS). In the EC/ Fe^{3+} /PDS system, Fe^{2+} could be regenerated from Fe^{3+} reduction at the cathode (Equation (3)), reducing the addition of the Fe concentration. Moreover, $\text{SO}_4^{\bullet-}$ could be generated in the electrochemical system by an electron transfer reaction of PDS (Equation (4)). Meanwhile, $\bullet\text{OH}$ could be produced on the surface of the dimensionally stable anode (DSA) (Equation (5)), enhancing the degradation process [25].



Previous studies have demonstrated IBU removal in the Fe/PS system or in the electro-oxidation system [26–28]. However, to the best of our knowledge, the system of electro-oxidation combined with Fe/PDS has never been applied to the degradation of IBU. It is expected that the coupling system would overcome the disadvantages of the Fe/PDS system, and reduce the reaction time of electro-oxidation, leading to lower energy consumption. Noteworthy, abundant inorganic anions (HCO_3^- , Cl^- , NO_3^- , H_2PO_4^-) and humic acids (HA) as natural organic matter (NOM) exist in water and waste water. Nevertheless, the effect of these co-existing substances on IBU removal in the processes based on the electrochemical technology, especially in the EC/ Fe^{3+} /PDS system, was rarely mentioned in the previous literature, limiting their application in the aquatic environment.

Therefore, the objective of this study was to supplement the knowledge gaps as aforementioned. Firstly, the feasibility of IBU degradation using the EC/ Fe^{3+} /PDS system was determined and the influencing factors of current density, PDS concentration, Fe^{3+} concentration, initial IBU concentration, initial pH, inorganic anions and humic acid on the degradation of IBU were systematically explored. Additionally, the degradation kinetics were also investigated. Moreover, the reaction by-products of IBU and major reactive oxygen species involved in the EC/ Fe^{3+} /PDS system were determined. Finally, the reaction mechanism of the EC/ Fe^{3+} /PDS system and IBU degradation pathways were proposed.

2. Results and Discussion

2.1. Comparative Study of Different Processes

IBU removal was carried out in various processes: PDS alone, electro-oxidation (EC), EC/PDS, the Fe^{3+} /PDS process, EC/ Fe^{3+} and EC/ Fe^{3+} /PDS system (Figure 1). The kinetic model of the EC/ Fe^{3+} /PDS system for IBU degradation was investigated by the pseudo-first-order according to Equation (6) [29].

$$\ln \frac{C}{C_0} = -kt \quad (6)$$

where k represents the rate constant for IBU removal, min^{-1} ; C_0 refers to the initial IBU concentration and C_t refers to the IBU concentration at time t , mg/L ; t is the reaction time, min . As shown in Table 1, the degradation kinetics of IBU obeyed the pseudo-first-order model according to the correlation coefficient values ($R^2 > 0.97$). As illustrated in Figure 1, PDS alone could hardly oxidize IBU, and the remaining PDS accounted for 98.0% of the initial PDS concentration. The reason was that PDS was stable and the oxidation capability of PDS was limited ($E_0 = 2.01$) at an ambient temperature [21,30]. The IBU removal in the Fe^{3+} /PDS process was nearly the same as that in the presence of PDS alone, and the remaining percentage of PDS was 97.6%, indicating that Fe^{3+} could hardly activate PDS to generate reactive radicals. A previous study also reported the low effectiveness of the Fe^{3+} /PDS system in iohexol degradation [31]. In the EC process, about 50.91% of IBU was eliminated and the k value was 0.0120 min^{-1} . The result of cyclic voltammograms for $\text{RuO}_2\text{-IrO}_2/\text{Ti}$ was shown in Figure 2. As observed, no obvious oxidation or reduction peaks could be identified. This phenomenon indicated that the degradation of IBU was attributed to the indirect oxidation process by $\bullet\text{OH}$ formed by water discharge at the surface of the DSA anode [25]. The introduction of Fe^{3+} into the electro-oxidation process formed the electro-Fenton (EF) reaction, and generated little amounts of $\bullet\text{OH}$, accelerating the IBU removal [32]. However, these hydroxyl radicals were insufficient to completely degrade IBU over a 60 min reaction. The combination of EC and PDS slightly improved the removal of IBU (60.12%) due to the $\text{SO}_4^{\bullet-}$ generated through the reaction of electron transfer (Equation (4)). In this case, the remaining percentage of PDS was 69.5%. Remarkably, the removal of IBU achieved 90.91% and the residual percent of PDS was 46.1% in the EC/ Fe^{3+} /PDS system. This was because Fe^{2+} could be formed by the cathodic reduction of Fe^{3+} , and then sulfate radicals could be continuously formed by the reaction between Fe^{2+} and PDS, thus enhancing the degradation process.

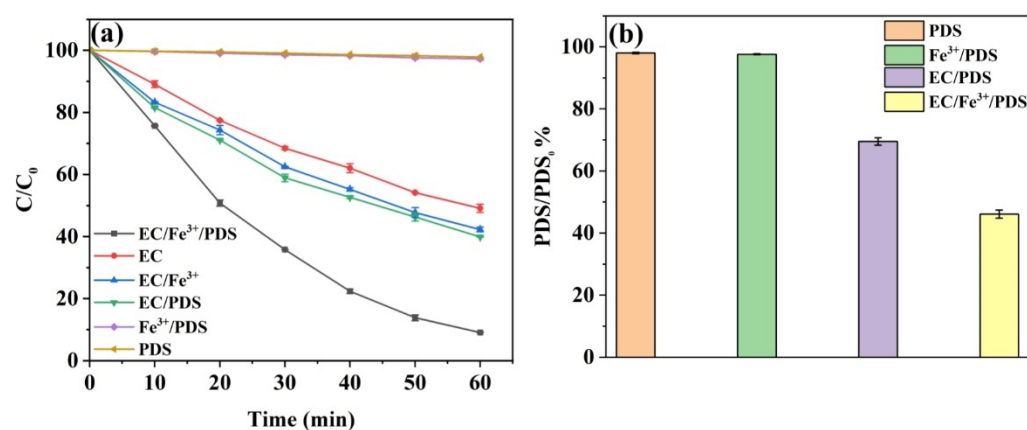
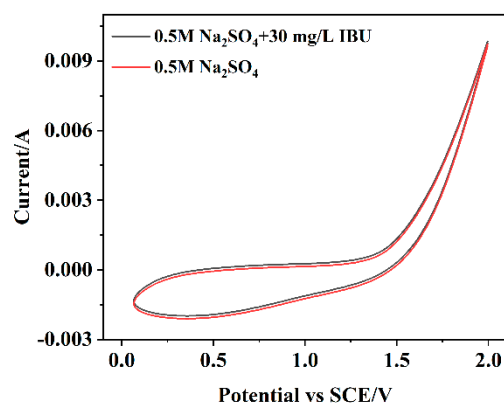


Figure 1. IBU removal (a) and remaining percentage of PDS (b) under different systems; ((initial IBU concentration) = 30 mg/L , (Fe^{3+} concentration) = 1 mM , (PDS concentration) = 8 mM , current density = 15 mA/cm^2 , initial $\text{pH} = 3$).

Table 1. The kinetics for IBU degradation in the EC/Fe³⁺/PDS system.

Parameters		k (min ⁻¹)	Half-Life (t _{1/2} , min)	R ²
Degradation under different systems	EC/Fe ³⁺ /PDS	0.0408	16.99	0.994
	EC	0.0120	57.76	0.998
	EC/Fe ³⁺	0.0143	48.47	0.997
	EC/PDS	0.0150	46.21	0.994
PDS concentration (mM)	6	0.0215	32.24	0.996
	8	0.0408	16.99	0.994
	10	0.0482	14.38	0.994
	12	0.0508	13.64	0.995
	14	0.0457	15.17	0.994
Fe ³⁺ concentration (mM)	0.5	0.0255	27.18	0.988
	1.0	0.0508	13.64	0.995
	1.5	0.0598	11.59	0.997
	2.0	0.0851	8.15	0.983
	2.5	0.0657	10.55	0.995
Current density (mA/cm ²)	5	0.0193	35.91	0.993
	10	0.0364	19.04	0.996
	15	0.0851	8.15	0.983
	20	0.0829	8.36	0.979
IBU concentration (mg/L)	30	0.0851	8.15	0.983
	40	0.0507	13.67	0.993
	50	0.0356	19.47	0.986
	60	0.0277	25.02	0.981
pH	3	0.0851	8.15	0.983
	5	0.0640	10.83	0.987
	7	0.0465	14.91	0.982
	9	0.0345	20.09	0.987

**Figure 2.** Cyclic voltammograms of RuO₂-IrO₂/Ti in 0.5 mol/L Na₂SO₄ solutions in the presence and absence of IBU (30 mg/L) at a scan rate of 10 mV/s.

2.2. Impact Factors

2.2.1. The Effect of PDS Concentration

PDS is the main source for the generation of SO₄^{•-}. Thus, the influence of initial PDS concentration on IBU removal efficiency was displayed in Figure 3a. The IBU removal raised gradually from 73.45% to 94.91% with the PDS concentration increasing from 6 to 12 mM, and the *k* value increasing from 0.0215 min⁻¹ to 0.0508 min⁻¹. However, the removal of IBU declined to 93.37% as the PDS concentration further increased. Previous studies have also reported that raising the PDS concentration to a certain value could generate more reactive radicals [33,34], resulting in acceleration of the decomposition of IBU. Whereas, in accordance with the literature [35,36], excessive addition of PDS could

reduce the degradation efficiency due to the self-quenching reactions of reactive radicals as well as their reaction with PDS (Equations (7)–(11)). Therefore, 12 mM was used as an optimum value of PDS for the downstream experiments.

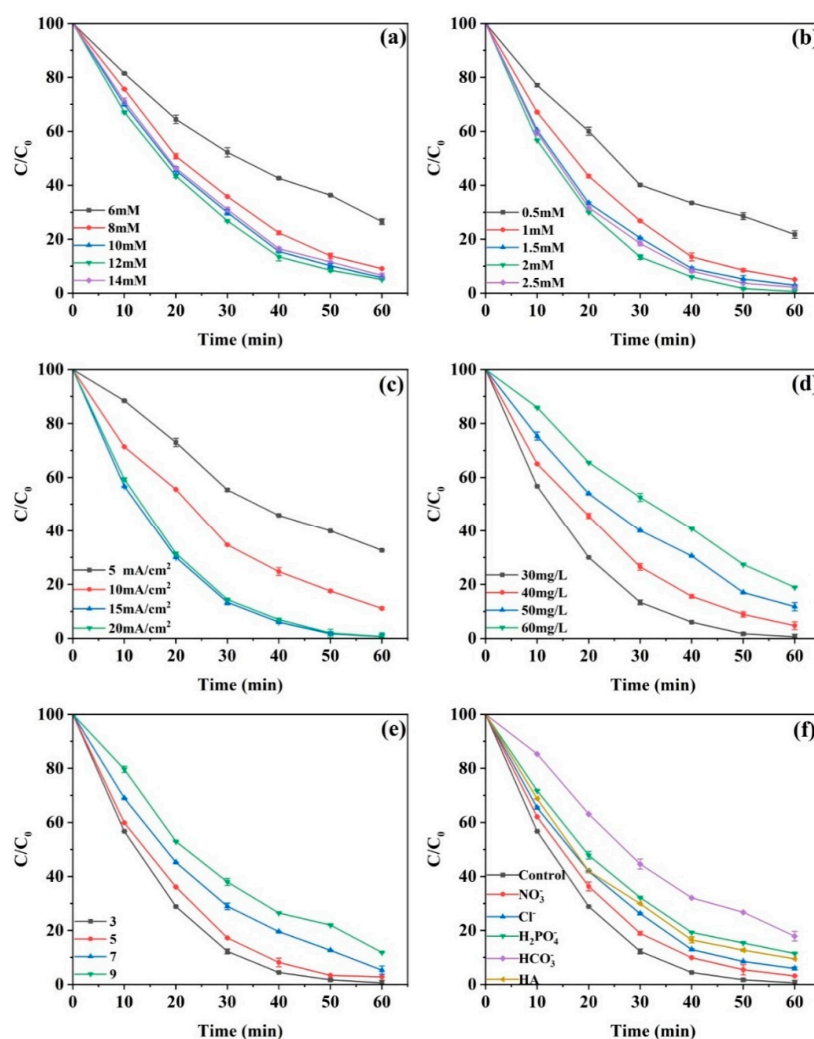
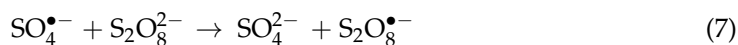
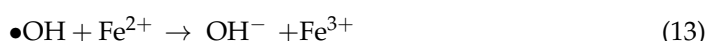
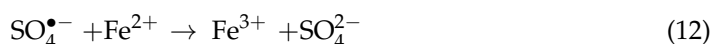


Figure 3. Effect of PDS concentration (a), Fe^{3+} concentration (b), current density (c), initial IBU concentration (d), initial pH (e), inorganic anions and HA (f) on IBU removal. ((initial IBU concentration) = 30 mg/L, (Fe^{3+} concentration) = 1 mM, current density = 15 mA/cm², initial pH = 3; (initial IBU concentration) = 30 mg/L, (PDS concentration) = 12 mM, current density = 15 mA/cm², initial pH = 3; (initial IBU concentration) = 30 mg/L, (Fe^{3+} concentration) = 2 mM, (PDS concentration) = 12 mM, initial pH = 3; (Fe^{3+} concentration) = 2 mM, (PDS concentration) = 12 mM, current density = 15 mA/cm², initial pH = 3; (initial IBU concentration) = 30 mg/L, (Fe^{3+} concentration) = 2 mM, (PDS concentration) = 12 mM, current density = 15 mA/cm²; (initial IBU concentration) = 30 mg/L, (Fe^{3+} concentration) = 2 mM, (PDS concentration) = 12 mM, current density = 15 mA/cm², initial pH = 3).

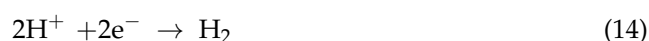
2.2.2. The Effect of the Initial Fe³⁺ Concentration

The influence of the Fe³⁺ concentration on the degradation of IBU was performed (Figure 3b). Increasing the Fe³⁺ concentration from 0.5 mM to 2 mM meant the IBU removal increased from 78.24% to 99.37%, while the *k* value augmented from 0.0255 min⁻¹ to 0.0851 min⁻¹. The upward trend of removal efficiency implied that increasing Fe³⁺ could generate more Fe²⁺ to activate PDS to degrade the IBU molecules. The continuing increase in the Fe³⁺ concentration up to 2.5 mM caused a slight decrease in IBU removal (97.83%) as well as the *k* value (0.0657 min⁻¹). This result could be attributed to the scavenging of reactive radicals by the redundant Fe²⁺ (Equations (12) and (13)).



2.2.3. The Effect of Current Density

As is well known, in the electrochemical process, current density plays a vital role in organic contaminant degradation. The influence of current density (5–20 mA/cm²) was investigated and displayed in Figure 3c. By raising the current density from 5 mA/cm² to 15 mA/cm², the IBU removal increased from 67.33% to 99.37%, and the *k* value increased progressively from 0.0193 min⁻¹ to 0.0851 min⁻¹. Higher current density would enhance the cathodic reduction of Fe³⁺ according to Equation (3), and then accelerate the decomposition of PDS to form active radicals [37]. Moreover, at the cathode, higher current density would strengthen the electron transfer to activate PDS, resulting in more generation of sulfate radicals. Meanwhile, higher current density promoted the generation of hydroxyl radicals at the anode. However, the removal of IBU and *k* value dropped to 99.30% and 0.0829 min⁻¹, respectively, as the current density further increased to 20 mA/cm². This phenomenon was attributed to the occurrence of side reactions initiated by the higher current density, such as the reaction of H₂ evolution at the cathode (Equation (14)) and O₂ evolution at the anode (Equation (15)) [32,38,39]. These side reactions would compete with the IBU removal, PDS activation and Fe³⁺ reduction.



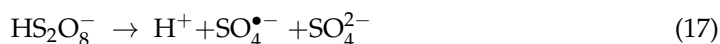
2.2.4. The Effect of the Initial IBU Concentration

The IBU removal and the *k* value gradually decreased with the increment of its concentration (Figure 3d). This result was in accordance with the finding of Shen et al. [9]. As the initial IBU concentration was elevated from 30 mg/L to 60 mg/L, the IBU removal and the *k* value reduced from 99.37% and 0.0851 min⁻¹ to 81.07% and 0.0277 min⁻¹, respectively. The reactive radicals generated were relatively stable when the PDS concentration, Fe³⁺ dosage and current density were fixed. However, higher amounts of intermediates could be formed at higher initial IBU concentration, which would compete for reactive radicals with the IBU molecules, slowing the decomposition of the IBU.

2.2.5. The Effect of the Initial pH

As displayed in Figure 3e, the influence of solution pH on IBU removal was carried out in the range of 3–9. The IBU removal dropped from 99.37% to 88.12% as the pH increased from 3 to 9, correspondingly, the *k* value dropped from 0.0851 min⁻¹ to 0.0345 min⁻¹. Clearly, an acidic pH facilitated the removal of IBU in this system, which agreed with that of recent studies via the EC/Fe/PS system [40,41]. The phenomenon was interpreted by the following aspects. In acidic conditions, the presence of H⁺ enhanced the formation of sulfate radicals in accordance with Equations (16) and (17) [42]. On the other hand, at higher pH levels, ferrous ions can be precipitated in the formation of ferric hydroxide, leading to the decrease in soluble Fe²⁺, thereby suppressing the activation of PDS [43].

In addition, under alkaline conditions, the $\text{SO}_4^{\bullet-}$ could convert to $\bullet\text{OH}$ by reacting with OH^- . The lifetime of $\bullet\text{OH}$ was shorter in comparison with $\text{SO}_4^{\bullet-}$. In addition, the standard oxidation potential of $\bullet\text{OH}$ was 2.7 V under acidic conditions, while the standard oxidation potential of $\bullet\text{OH}$ was only 1.8 V with neutral conditions [44], indicating that the oxidation ability of $\bullet\text{OH}$ was stronger at a lower pH level.



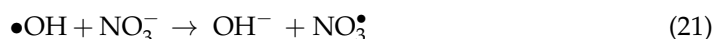
2.2.6. Effect of Co-Existing Components

It should be noted that the water and waste water had abundant inorganic anions (HCO_3^- , Cl^- , NO_3^- , H_2PO_4^-) and humic acids (HA) as natural organic matter (NOM). Hence, it is of great importance to investigate their effects on IBU removal in the EC/ Fe^{3+} /PDS system. The experiments were performed with 10 mM inorganic anions and 10 mg/L HA, respectively (Figure 3f). Inorganic anions inhibited the IBU removal, and the inhibitive effect of inorganic anions on IBU removal kept the ascending order: $\text{HCO}_3^- > \text{H}_2\text{PO}_4^- > \text{Cl}^- > \text{NO}_3^-$. After introducing 10 mM of HCO_3^- , H_2PO_4^- , Cl^- and NO_3^- , the removal of IBU reduced to 82.11%, 88.50%, 94.07% and 96.83%, respectively.

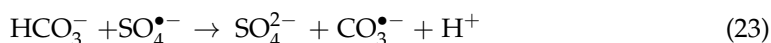
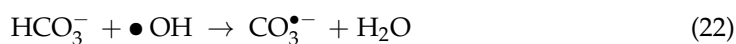
At the anode, Cl^- could be oxidized to free chlorine (e.g., HClO , ClO^-) with weaker oxidation capacity. This was a side reaction compared with the production of $\bullet\text{OH}$ at the anode. Cl^- could consume $\text{SO}_4^{\bullet-}$ and $\bullet\text{OH}$ to form less reactive radicals ($\text{Cl}\bullet$ and $\text{HOCl}^{\bullet-}$) ((Equations (18) and (19)) [45]. As previous reports demonstrate, the occurrence of complexation reactions of Cl^- with Fe^{3+} and Fe^{2+} generated FeCl^{2+} , FeCl^+ , etc, reducing the concentration of Fe^{2+} and Fe^{3+} [46], and consequently weakening the removal of IBU.



There are two reasons for a slightly decreasing trend caused by NO_3^- . (1) NO_3^- could compete with IBU for the $\bullet\text{OH}$ and $\text{SO}_4^{\bullet-}$, leading to the formation of some inactive radicals ((Equations (20) and (21)) [47]; (2) The addition of NO_3^- increased the ion strength of the solution, resulting in a slower decomposition of PDS.



The inhibition of HCO_3^- could be explained as follows: the reaction of $\bullet\text{OH}$ and $\text{SO}_4^{\bullet-}$ with HCO_3^- , leading to the production of less reactive radical ($\text{CO}_3^{\bullet-}$) ((Equations (22) and (23)) [48]. (2) HCO_3^- could affect the involved oxidation reactions by changing the solution pH. As discussed above, increasing the pH had a negative effect on the oxidation process.



The negative effect of H_2PO_4^- was related to the scavenging effect ((Equations (24) and (25)) [49]. In addition, the formation of H_2PO_4^- -Fe complexes species decreased the active iron ions, inducing inhibition of the degradation process.



Besides the inorganic anions, the HA had a detrimental influence on IBU removal. The removal of IBU decreased from 99.37% to 90.50% after the addition of 10 mg/L HA.

HA, rich in carboxyl and hydroxyl functional groups, usually acts as a scavenger of $\text{SO}_4^{\bullet-}$ and $\bullet\text{OH}$ due to the high reactivity towards $\bullet\text{OH}$ ($k_{\bullet\text{OH}/\text{HA}} = 1.39 \times 10^8 \text{ M}^{-1}\text{S}^{-1}$) and $\text{SO}_4^{\bullet-}$ ($k_{\text{SO}_4^{\bullet-}/\text{HA}} = 7.8 \times 10^7 \text{ M}^{-1}\text{S}^{-1}$) [50,51]. Aside from the ability to quench radicals, it is easier to seize the dissolved Fe^{2+} and Fe^{3+} owing to the feature of a strong ligand, leading to the decrease in IBU removal [52].

Overall, the effects of inorganic ions and HA on the IBU degradation should be adequately considered.

2.3. Comparison with Other Technologies

The energy consumption of the EC/process was assessed by the electrical efficiency per log order (EE/O) according to Equation (26) [53].

$$\text{EE/O (Wh/L)} = \frac{U \times I \times t}{V \times \log\left(\frac{C_0}{C_t}\right)} \quad (26)$$

where U is the recorded average electrolysis voltage (V), V is volume (L), I is the electrolysis current (A), t is the electrolysis time (h).

Moreover, the energy efficiency was estimated by Equation (27) [54].

$$\text{Energy efficiency (mg/Wh)} = \frac{m}{U \times I \times t} \quad (27)$$

where U is the recorded average electrolysis voltage (V), I is the electrolysis current (A), t is the electrolysis time (h), m is the amount of contaminant degraded (mg).

The EE/O of the EC/ Fe^{3+} /PDS process was 2.79 Wh/L, which was lower than the EE/O for electro-oxidation of IBU by Ti/SnO₂-Sb/Ce-PbO₂ (4.3–30.6 Wh/L) [2]. Moreover, the energy efficiency was 8.15 mg/Wh in our study, which was much higher than the decomposition of IBU by ozonation (2.15 mg/Wh) or by DBD plasma (2.5 mg/Wh) [55]. Moreover, the degradation performance of the EC/ Fe^{3+} /PDS system was compared with other technologies. As can be seen from Table 2, the EC/ Fe^{3+} /PDS system performed better in IBU removal than other methods, indicating that the EC/ Fe^{3+} /PDS system is a potential technology for IBU degradation in water.

Table 2. Comparison with other technologies for IBU degradation.

Technology	Experimental Conditions	IBU Removal (%)	Reference
Electro-oxidation (Ti/SnO ₂ -Sb/Ce-PbO ₂)	V = 30 mL; IBU = 20 mg/L; current density = 10 mA/cm ²	90% removal in 60 min	[2]
BaTiO ₃ /PDS under ultrasonic-wave	V = 25 mL, PS = 1.0 mM, IBU = 6.0 mg/L, BaTiO ₃ = 2.0 g/L	99% removal in 60 min	[7]
Electro-Fenton	V = 200 mL, IBU = 10 mg/L, pH = 3.0, Fe ²⁺ = 0.7 mM	94.8% removal in 150 min	[56]
UV/H ₂ O ₂	IBU = 10 μM, H ₂ O ₂ = 0.5 mM, pH = 5.2	95% removal in 240 min	[57]
Photo-Fenton (HSO ₃ -MIL-53(Fe))	V = 50 mL, IBU = 10 mg/L, H ₂ O ₂ = 20 mM, HSO ₃ -MIL-53(Fe) = 200 mg/L, pH ₀ = 8.0	100% removal in 90 min	[58]
Photocatalysis (phosphorus and sulfur co-doped graphitic carbon nitride (PSGCN) and AgBr particle)	Photocatalyst = 100 mg/100 mL, IBU = 15 mg/L	90% removal in 100 min	[59]
EC/ Fe^{3+} /PDS	V = 200 mL; pH = 3; IBU = 30 mg/L; current density = 10 mA/cm ² ; Fe ³⁺ = 2.0 mM; PDS = 12 mM	99.37% removal in 60 min	this work

2.4. Determination of Reactive Species

Quenching experiments were conducted to determine the generation of reactive radicals. Methanol (MA) was utilized as a capturer for both $\text{SO}_4^{\bullet-}$ and $\bullet\text{OH}$, as it had similar quenching rate with $\bullet\text{OH}$ ($k_{\bullet\text{OH}/\text{MA}} = 9.7 \times 10^8 \text{ M}^{-1}\text{S}^{-1}$) and $\text{SO}_4^{\bullet-}$ ($k_{\text{SO}_4^{\bullet-}/\text{MA}}$

$1.61 \times 10^7 \text{ M}^{-1}\text{S}^{-1}$) [60,61]. Tert-butyl alcohol (TBA) was regarded as $\bullet\text{OH}$ scavenger ($k_{\bullet\text{OH}/\text{TBA}} 9.7 \times 10^8 \text{ M}^{-1}\text{S}^{-1}$) as its rate constant with $\bullet\text{OH}$ was approximately 1000-fold times than that for $\text{SO}_4^{\bullet-}$ [62]. As displayed in Figure 4, both MA and TBA inhibited IBU removal. Specifically, the removal of IBU reached 99.37%, whereas it decreased to 29.36% and 63.92% after the addition of MA and TBA. The result indicated that both $\text{SO}_4^{\bullet-}$ and $\bullet\text{OH}$ participated in the process, and the contribution of $\text{SO}_4^{\bullet-}$ and $\bullet\text{OH}$ for IBU degradation in the EC/ Fe^{3+} /PDS system was almost equal.

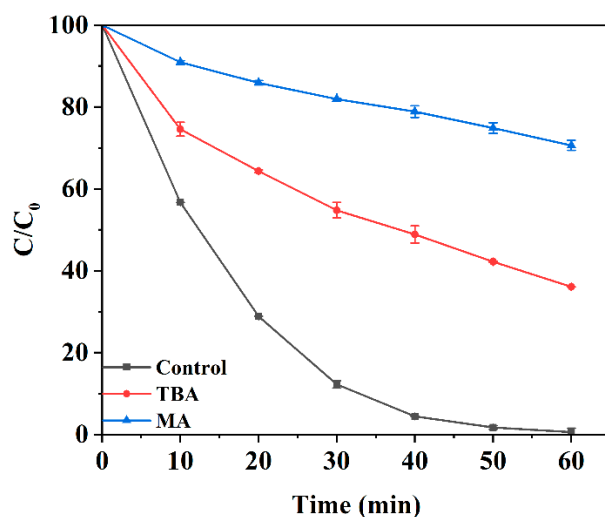


Figure 4. Effect of TBA and MA on IBU degradation. ((initial IBU concentration) = 30 mg/L, (Fe^{3+} concentration) = 2 mM, (PDS concentration) = 12 mM, current density = 15 mA/cm², initial pH = 3, (MA concentration) = 500 mM, (TBA concentration) = 500 mM).

2.5. Proposed Mechanism of the EC/ Fe^{3+} /PDS Process

According to the results and previous reports, the reaction mechanism of the EC/ Fe^{3+} /PDS process was proposed (Figure 5). Fe^{2+} could be reproduced from the reduction of Fe^{3+} at the cathode, and then activated PDS to produce $\text{SO}_4^{\bullet-}$. What is more, $\text{SO}_4^{\bullet-}$ could be generated by an electron transfer reaction. Additionally, $\bullet\text{OH}$ could be produced on the surface of the DSA anode, enhancing the degradation process. $\text{SO}_4^{\bullet-}$ could be converted to $\bullet\text{OH}$ by reacting with H_2O and OH^- . Finally, IBU was degraded to CO_2 and H_2O by the oxidation of both $\text{SO}_4^{\bullet-}$ and $\bullet\text{OH}$.

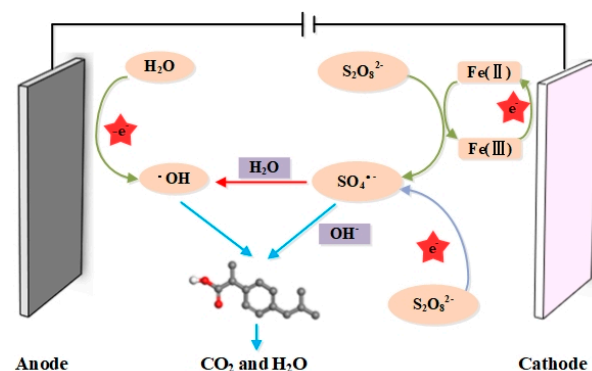


Figure 5. Reaction mechanism of the EC/ Fe^{3+} /PDS system.

2.6. Oxidation Products and Proposed Pathway of IBU Degradation

The degradation intermediates of IBU were identified using LC-MS/MS. Consequently, a total of seven intermediates were determined (Figure 6). The chemical structure, reaction time, molecular formula and weight of IBU degradation products were summarized in Table 3, and the oxidation pathways of IBU degradation were presented in Figure 7.

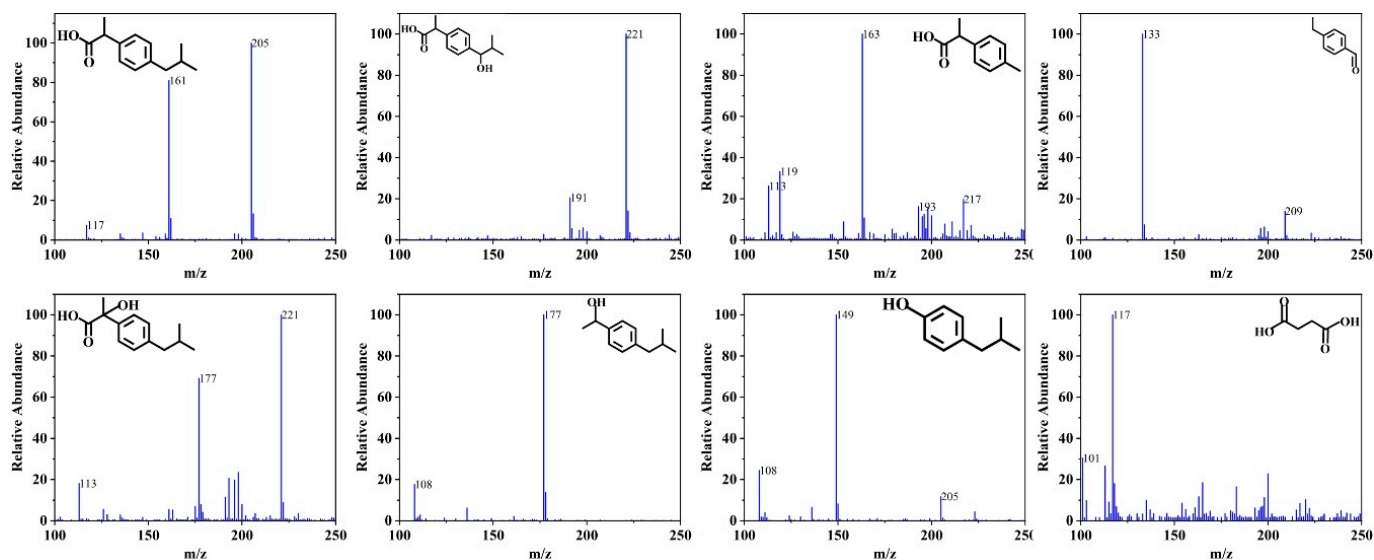


Figure 6. Mass spectra of the products generated during the degradation of IBU in EC/Fe³⁺/PDS system.

Table 3. Main intermediates for the degradation of IBU in the EC/Fe³⁺/PDS system.

Product	Reaction Time	Molecular Weight	Chemical Structure
IBU	6.24	206	
P1	5.26	222	
P2	2.81	164	
P3	3.40	134	
P4	5.36	222	
P5	6.54	178	
P6	7.53	150	
P7	8.52	118	

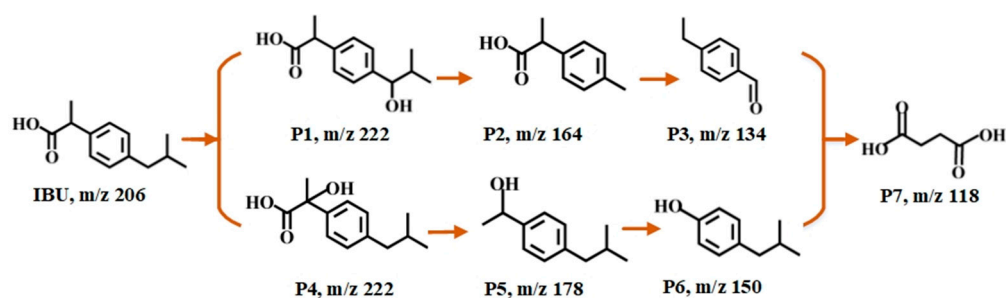


Figure 7. Degradation pathways of IBU in the EC/Fe³⁺/PDS system.

The attack of $\bullet\text{OH}$ at different side chains of the IBU molecular formation produced product 1 (m/z, 222) and product 4 (m/z, 222). It is noteworthy that hydroxylated ibuprofen was commonly observed in the process of IBU degradation [63,64]. In the pathway I, the side chains of product 1 (m/z, 222) could be subsequently separated from the benzene ring, followed by oxidation reactions for the formation of product 2 (m/z, 164) [65]. Product 2 (m/z, 164) could be transformed to product 3 (m/z, 134) via the decarboxylation. For pathway II, product 4 (m/z, 222) underwent the decarboxylation of the side chains, resulting in the generation of the product 5 (m/z, 178). Then, the dehydration and hydroxylation occurred on the side chain of the benzene ring of product 5 (m/z, 178), leading to the production of product 6 (m/z, 150). With the continuous oxidation reaction, the aromatic rings of product 3 (m/z, 134) and product 6 (m/z, 150) opened, resulting in the formation of product 7 (m/z 118). Finally, products 7 could be easily oxidized to CO_2 and H_2O [66].

3. Materials and Methods

3.1. Materials

Ibuprofen and sodium persulfate ($\text{Na}_2\text{S}_2\text{O}_8$) were obtained from Sigma-Aldrich Chemical Co., Ltd. HPLC grade acetonitrile, methanol, formic acid and acetic acid were bought from Sinopharm Chemical Reagent Beijing Co., Ltd. Sulfuric acid (H_2SO_4), sodium hydroxide (NaOH), sodium sulfate (Na_2SO_4), Ferric sulfate ($\text{Fe}_2(\text{SO}_4)_3$), sodium chloride (NaCl), sodium dihydrogen phosphate (NaH_2PO_4), sodium bicarbonate (NaHCO_3), sodium nitrate (NaNO_3), tert-butanol and acetonitrile were obtained from Xilong Science Co., Ltd. $\text{RuO}_2\text{-IrO}_2/\text{Ti}$ mesh and Ti plate electrode were bought from Beijing Hengli Ti Co., Ltd., China. All chemicals were analytic-grade. All aqueous solutions were prepared with Millipore water (18 M Ω cm).

3.2. Analytical Methods

IBU concentration was determined using a high-performance liquid chromatography system (LC-20AT, Shimadzu, Japan) with a chromatographic separation of an Inertsil ODS-3 C18 column (250 mm \times 4.6 mm, 5 μm). The UV-visible detector was set at 220 nm. A mixture of 63:37 (v/v) acetonitrile/water (containing 0.1% acetic acid) was used as the mobile phase, at a flow rate of 1.0 mL/min. The byproducts were analyzed with a Waters Acquity UPLC-QTOF-MS/MS (Xevo G2) system, operating in a negative ion mode with an electrospray ionization source. A Waters Acquity UPLC BEH C18 column (50 mm \times 2.1 mm, 1.7 μm) was used to separate chromatograph. The mobile phase was composed of acetonitrile (A) and water containing 0.1% formic acid (B), with 0.3 mL/min flow rate. Component B was maintained at 10% during the first 1 min, then B was changed to 100% in 1–10 min. Finally, component B returned to 10% during the last 2 min.

The degradation efficiency is calculated by the Equation (28) [67].

$$\text{Degradation efficiency} = \frac{C_0 - C_t}{C_0} \quad (28)$$

where C_0 refers to the initial IBU concentration and C_t refers to the IBU concentration at time t , mg/L.

3.3. Experimental Procedure

The removal of IBU was performed in an undivided 250 mL glass beaker which contained 200 mL of IBU solution. The glass beaker was immersed in a water bath to keep the temperature constant at 25 °C. The reaction solution was mixed continuously with a magnetic stirrer. The schematic of EC/Fe³⁺/PDS system was shown in Figure 8. A RuO₂-IrO₂/Ti mesh (3 cm × 5 cm) was applied as anode while Ti plate (3 cm × 5 cm) was served as cathode. 0.05 mol/L Na₂SO₄ was applied as supporting electrolyte. Ferric sulfate (Fe₂(SO₄)₃) was employed to provide Fe³⁺ to avoid the interference of other anions. The distance between the anode and the cathode was maintained as 1.5 cm. The solutions were unbuffered to avoid the quenching effect of buffers, and the initial pH of the IBU solution was adjusted with H₂SO₄ and NaOH (0.1 mol/L) and measured with a pH meter (FE28-CN, Mettler Toledo). A digital DC power (DH1718E-5, 35 V, 5 A, Dahua Electronic Co., Beijing, China) was used to provide constant electric current for electrochemical experiments. After addition of a certain amount of PDS and Fe³⁺ solution, the DC power supply was started immediately. Periodically, reaction solution samples (2 mL) were withdrawn and directly filtered using a 0.45 μm microfiltration membrane and quenched with methanol before analysis. All the experiments were performed in triplicate.

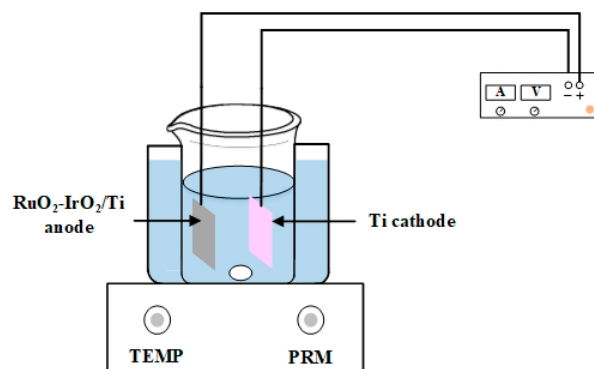


Figure 8. Schematic of the EC/Fe³⁺/PDS system.

The cyclic voltammetry was performed using an electrochemical workstation (Chenhua, CHI 660, China) equipped with a typical three-electrode system. The Ti (10 mm × 20 mm) was used as the working electrode. A platinum plate (10 mm × 20 mm) was employed as the counter electrode. The Ag/AgCl electrode was employed as the reference electrode. The cyclic voltammetry experiment was conducted at room temperature with the absence and presence of 30 mg/L IBU in 0.5 mol/L Na₂SO₄. The scan rate was set at 10 mV/s.

4. Conclusions

An electro-assisted Fe³⁺/PDS process (EC/Fe³⁺/PDS) was investigated for IBU degradation in an aqueous solution. The combination of Fe³⁺/PDS and electro-oxidation was displayed to be effective to degrade IBU. The synergistic effect was attributed to the following aspects: (1) the electro-oxidation; (2) sulfate radicals generated from the activation of PDS by ferrous ions formed via cathodic reduction; (3) sulfate radicals generated from the electron transfer reaction. Free radicals quenching experiments revealed that both SO₄^{•−} and •OH contributed to the excellent removal of IBU. Based on the above analysis, the enhanced catalytic mechanism was also elucidated. Furthermore, increasing the current density (5–15 mA/cm²), PDS concentration (6–12 mM) or Fe³⁺ concentration (0.5–2 mM) enhanced the IBU degradation while a slight inhibitory effect was obtained with a further increase in these parameters. Compared with neutral and alkaline conditions, an acidic pH facilitated the IBU degradation. Moreover, the removal of IBU decreased with increasing the initial IBU concentration. All degradation processes of IBU in the system followed the pseudo-first order reaction kinetic models. At optimum conditions ((Fe³⁺ concentration) = 2.0 mM, (PDS concentration) = 12 mM, (initial IBU concentration)

= 30 mg/L, current density = 15 mA/cm², initial pH = 3), IBU removal and the *k* value reached 99.37% and 0.0851 min⁻¹ within a 60 min reaction. Furthermore, inorganic anions and HA inhibited the degradation of IBU. Finally, seven intermediates were determined by LC-MS/MS analysis, and a plausible IBU degradation route was suggested.

Author Contributions: Conceptualization, C.S. and N.Q.; methodology, Y.L., X.L. and X.W.; validation, Y.L., G.J. and J.Q.; formal analysis, G.J. and J.Q.; data curation, C.S. and N.Q.; writing—original draft preparation, C.S. and N.Q.; writing—review and editing, X.L., C.S. and N.Q.; supervision, X.L., G.J. and J.Q.; funding acquisition, C.S., X.W. and X.L. All authors have read and agreed to the published version of the manuscript.

Funding: This research was funded by the Natural Science Foundation of Shandong Province, China (ZR2019PB031), the Doctoral Research Initiation Fund of Zaozhuang University (1020706 and 1020711) and the Open Foundation of Key Laboratory for Water and Sediment Science, Ministry of Education, Beijing Normal University (SS202104).

Data Availability Statement: Data is contained within the article.

Conflicts of Interest: The authors declare no conflict of interest.

References

1. Parolini, M. Toxicity of the Non-Steroidal Anti-Inflammatory Drugs (NSAIDs) acetylsalicylic acid, paracetamol, diclofenac, ibuprofen and naproxen towards freshwater invertebrates: A review. *Sci. Total Environ.* **2020**, *740*, 140043. [CrossRef]
2. Wang, C.; Yu, Y.; Yin, L.; Niu, J.; Hou, L.-A. Insights of ibuprofen electro-oxidation on metal-oxide-coated Ti anodes: Kinetics, energy consumption and reaction mechanisms. *Chemosphere* **2016**, *163*, 584–591. [CrossRef] [PubMed]
3. Brillas, E. A critical review on ibuprofen removal from synthetic waters, natural waters, and real wastewaters by advanced oxidation processes. *Chemosphere* **2022**, *286*, 131849. [CrossRef] [PubMed]
4. Li, X.; Zhang, H.; Ma, F.; Cheng, S.; Shen, Z.; Zhang, J.; Min, J.; Wang, Y.; Liu, G.; Yao, H. Electro-catazone treatment of ozone-resistant drug ibuprofen: Interfacial reaction kinetics, influencing mechanisms, and degradation sites. *J. Hazard. Mater. Adv.* **2021**, *4*, 100023. [CrossRef]
5. Ding, H.; Hu, J. Degradation of ibuprofen by UVA-LED/TiO₂/persulfate process: Kinetics, mechanism, water matrix effects, intermediates and energy consumption. *Chem. Eng. J.* **2020**, *397*, 125462. [CrossRef]
6. Cao, J.; Lai, L.; Lai, B.; Yao, G.; Chen, X.; Song, L. Degradation of tetracycline by peroxymonosulfate activated with zero-valent iron: Performance, intermediates, toxicity and mechanism. *Chem. Eng. J.* **2019**, *364*, 45–56. [CrossRef]
7. Peng, F.; Yin, R.; Liao, Y.; Xie, X.; Sun, J.; Xia, D.; He, C. Kinetics and mechanisms of enhanced degradation of ibuprofen by piezo-catalytic activation of persulfate. *Chem. Eng. J.* **2020**, *392*, 123818. [CrossRef]
8. Zhang, G.; Ding, Y.; Nie, W.; Tang, H. Efficient degradation of drug ibuprofen through catalytic activation of peroxymonosulfate by Fe₃C embedded on carbon. *J. Environ. Sci.* **2019**, *78*, 1–12. [CrossRef]
9. Shen, C.; Wang, Y.; Fu, J. Urchin-like Co₃O₄ anchored on reduced graphene oxide with enhanced performance for peroxymonosulfate activation in ibuprofen degradation. *J. Environ. Manag.* **2022**, *307*, 114572. [CrossRef]
10. Zhu, M.; Zhang, M.; Yuan, Y.; Zhang, P.; Du, S.; Ya, T.; Chen, D.; Wang, X.; Zhang, T. Responses of microbial communities and their interactions to ibuprofen in a bio-electrochemical system. *J. Environ. Manag.* **2021**, *289*, 112473. [CrossRef]
11. Kristensen, D.M.; Desdoits-Lethimonier, C.; Mackey, A.L.; Dalgaard, M.D.; De Masi, F.; Munkbøl, C.H.; Styriehave, B.; Antignac, J.-P.; Le Bizec, B.; Platel, C.; et al. Ibuprofen alters human testicular physiology to produce a state of compensated hypogonadism. *Proc. Natl. Acad. Sci. USA* **2018**, *115*, E715. [CrossRef] [PubMed]
12. Leverrier-Penna, S.; Mitchell, R.T.; Becker, E.; Lecante, L.; Ben Maamar, M.; Homer, N.; Lavoué, V.; Kristensen, D.M.; Dejuqc-Rainsford, N.; Jégou, B.; et al. Ibuprofen is deleterious for the development of first trimester human fetal ovary ex vivo. *Hum. Reprod.* **2018**, *33*, 482–493. [CrossRef] [PubMed]
13. Geiger, E.; Hornek-Gausterer, R.; Saçan, M.T. Single and mixture toxicity of pharmaceuticals and chlorophenols to freshwater algae *Chlorella vulgaris*. *Ecotoxicol. Environ. Saf.* **2016**, *129*, 189–198. [CrossRef]
14. Ding, T.; Yang, M.; Zhang, J.; Yang, B.; Lin, K.; Li, J.; Gan, J. Toxicity, degradation and metabolic fate of ibuprofen on freshwater diatom *Navicula* sp. *J. Hazard. Mater.* **2017**, *330*, 127–134. [CrossRef] [PubMed]
15. Gong, H.; Chu, W.; Huang, Y.; Xu, L.; Chen, M.; Yan, M. Solar photocatalytic degradation of ibuprofen with a magnetic catalyst: Effects of parameters, efficiency in effluent, mechanism and toxicity evolution. *Environ. Pollut.* **2021**, *276*, 116691. [CrossRef] [PubMed]
16. Wang, Y.; Shen, C.; Li, L.; Li, H.; Zhang, M. Electrocatalytic degradation of ibuprofen in aqueous solution by a cobalt-doped modified lead dioxide electrode: Influencing factors and energy demand. *RSC Adv.* **2016**, *6*, 30598–30610. [CrossRef]
17. Yang, Z.; Su, R.; Luo, S.; Spinney, R.; Cai, M.; Xiao, R.; Wei, Z. Comparison of the reactivity of ibuprofen with sulfate and hydroxyl radicals: An experimental and theoretical study. *Sci. Total Environ.* **2017**, *590–591*, 751–760. [CrossRef]

18. Shen, X.; Zhu, Z.; Zhang, H.; Di, G.; Chen, T.; Qiu, Y.; Yin, D. Carbonaceous composite materials from calcination of azo dye-adsorbed layered double hydroxide with enhanced photocatalytic efficiency for removal of Ibuprofen in water. *Environ. Sci. Eur.* **2020**, *32*, 77. [[CrossRef](#)]
19. Naderi, M.; Soltani, R.D.C. Hybrid of ZnFe layered double hydroxide/nano-scale carbon for activation of peroxymonosulfate to decompose ibuprofen: Thermodynamic and reaction pathways investigation. *Environ. Technol. Innov.* **2021**, *24*, 101951. [[CrossRef](#)]
20. Wojnárovits, L.; Takács, E. Rate constants of sulfate radical anion reactions with organic molecules: A review. *Chemosphere* **2019**, *220*, 1014–1032. [[CrossRef](#)]
21. Zhou, Z.; Liu, X.; Sun, K.; Lin, C.; Ma, J.; He, M.; Ouyang, W. Persulfate-based advanced oxidation processes (AOPs) for organic-contaminated soil remediation: A review. *Chem. Eng. J.* **2019**, *372*, 836–851. [[CrossRef](#)]
22. Wang, Z.; Qiu, W.; Pang, S.; Gao, Y.; Zhou, Y.; Cao, Y.; Jiang, J. Relative contribution of ferryl ion species (Fe(IV)) and sulfate radical formed in nanoscale zero valent iron activated peroxydisulfate and peroxymonosulfate processes. *Water Res.* **2020**, *172*, 115504. [[CrossRef](#)] [[PubMed](#)]
23. Lin, H.; Wu, J.; Zhang, H. Degradation of clofibrac acid in aqueous solution by an EC/Fe³⁺/PMS process. *Chem. Eng. J.* **2014**, *244*, 514–521. [[CrossRef](#)]
24. Cui, Y.-H.; Lv, X.-D.; Lei, J.-X.; Liu, Z.-Q. Synergistic Effect of Cathode/peroxymonosulfate/Fe³⁺ on Phenol Degradation. *Electrochim. Acta* **2017**, *245*, 201–210. [[CrossRef](#)]
25. Lin, H.; Zhong, X.; Ciotonea, C.; Fan, X.; Mao, X.; Li, Y.; Deng, B.; Zhang, H.; Royer, S. Efficient degradation of clofibrac acid by electro-enhanced peroxydisulfate activation with Fe-Cu/SBA-15 catalyst. *Appl. Catal. B Environ.* **2018**, *230*, 1–10. [[CrossRef](#)]
26. Gong, H.; Chu, W.; Lam, S.H.; Lin, A.Y.-C. Ibuprofen degradation and toxicity evolution during Fe²⁺/Oxone/UV process. *Chemosphere* **2017**, *167*, 415–421. [[CrossRef](#)]
27. Liu, Y.; Zhang, Y.; Wang, B.; Wang, S.; Liu, M.; Wu, Y.; Lu, L.; Ren, H.; Li, H.; Dong, W.; et al. Degradation of ibuprofen in soil systems by persulfate activated with pyrophosphate chelated Fe(II). *Chem. Eng. J.* **2020**, *379*, 122145. [[CrossRef](#)]
28. Tran, N.; Drogui, P.; Nguyen, L.; Brar, S.K. Optimization of sono-electrochemical oxidation of ibuprofen in wastewater. *J. Environ. Chem. Eng.* **2015**, *3*, 2637–2646. [[CrossRef](#)]
29. Hunge, Y.M.; Uchida, A.; Tominaga, Y.; Fujii, Y.; Yadav, A.A.; Kang, S.-W.; Suzuki, N.; Shitanda, I.; Kondo, T.; Itagaki, M.; et al. Visible Light-Assisted Photocatalysis Using Spherical-Shaped BiVO₄ Photocatalyst. *Catalysts* **2021**, *11*, 460. [[CrossRef](#)]
30. Matzek, L.W.; Carter, K.E. Activated persulfate for organic chemical degradation: A review. *Chemosphere* **2016**, *151*, 178–188. [[CrossRef](#)]
31. Lv, X.-D.; Yang, S.-Q.; Xue, W.-J.; Cui, Y.-H.; Liu, Z.-Q. Performance of Cu-cathode/Fe³⁺/ peroxymonosulfate process on iohexol degradation. *J. Hazard. Mater.* **2019**, *366*, 250–258. [[CrossRef](#)] [[PubMed](#)]
32. Liu, J.; Zhong, S.; Song, Y.; Wang, B.; Zhang, F. Degradation of tetracycline hydrochloride by electro-activated persulfate oxidation. *J. Electroanal. Chem.* **2018**, *809*, 74–79. [[CrossRef](#)]
33. Zhen, J.; Zhang, S.; Zhuang, X.; Ahmad, S.; Lee, T.; Si, H.; Cao, C.; Ni, S.-Q. Sulfate radicals based heterogeneous peroxymonosulfate system catalyzed by CuO-Fe₃O₄-Biochar nanocomposite for bisphenol A degradation. *J. Water Process Eng.* **2021**, *41*, 102078. [[CrossRef](#)]
34. Chen, X.-L.; Li, F.; Zhang, M.; Liu, B.; Chen, H.; Wang, H. Highly dispersed and stabilized Co₃O₄/C anchored on porous biochar for bisphenol A degradation by sulfate radical advanced oxidation process. *Sci. Total Environ.* **2021**, *777*, 145794. [[CrossRef](#)]
35. Li, G.; Cao, X.-Q.; Meng, N.; Huang, Y.-M.; Wang, X.-D.; Gao, Y.-Y.; Li, X.; Yang, T.-S.; Li, B.-L.; Zhang, Y.-Z.; et al. Fe₃O₄ supported on water caltrop-derived biochar toward peroxymonosulfate activation for urea degradation: The key role of sulfate radical. *Chem. Eng. J.* **2021**, *433*, 133595. [[CrossRef](#)]
36. Babaei, A.A.; Golshan, M.; Kakavandi, B. A heterogeneous photocatalytic sulfate radical-based oxidation process for efficient degradation of 4-chlorophenol using TiO₂ anchored on Fe oxides@carbon. *Process Saf. Environ. Prot.* **2021**, *149*, 35–47. [[CrossRef](#)]
37. Chanikya, P.; Nidheesh, P.V.; Syam Babu, D.; Gopinath, A.; Suresh Kumar, M. Treatment of dyeing wastewater by combined sulfate radical based electrochemical advanced oxidation and electrocoagulation processes. *Sep. Purif. Technol.* **2021**, *254*, 117570. [[CrossRef](#)]
38. Qi, F.; Zeng, Z.; Wen, Q.; Huang, Z. Enhanced organics degradation by three-dimensional (3D) electrochemical activation of persulfate using sulfur-doped carbon particle electrode: The role of thiophene sulfur functional group and specific capacitance. *J. Hazard. Mater.* **2021**, *416*, 125810. [[CrossRef](#)]
39. Sun, X.; Liu, Z.; Sun, Z. Electro-enhanced degradation of atrazine via Co-Fe oxide modified graphite felt composite cathode for persulfate activation. *Chem. Eng. J.* **2021**, *433*, 133789. [[CrossRef](#)]
40. Bu, L.; Zhou, S.; Shi, Z.; Bi, C.; Zhu, S.; Gao, N. Iron electrode as efficient persulfate activator for oxcabazepine degradation: Performance, mechanism, and kinetic modeling. *Sep. Purif. Technol.* **2017**, *178*, 66–74. [[CrossRef](#)]
41. Aseman-Bashiz, E.; Sayyaf, H. Metformin degradation in aqueous solutions by electro-activation of persulfate and hydrogen peroxide using natural and synthetic ferrous ion sources. *J. Mol. Liq.* **2020**, *300*, 112285. [[CrossRef](#)]
42. Akbari, S.; Ghanbari, F.; Moradi, M. Bisphenol A degradation in aqueous solutions by electrogenerated ferrous ion activated ozone, hydrogen peroxide and persulfate: Applying low current density for oxidation mechanism. *Chem. Eng. J.* **2016**, *294*, 298–307. [[CrossRef](#)]
43. Wang, Y.R.; Chu, W. Degradation of 2,4,5-trichlorophenoxyacetic acid by a novel Electro-Fe(II)/Oxone process using iron sheet as the sacrificial anode. *Water Res.* **2011**, *45*, 3883–3889. [[CrossRef](#)] [[PubMed](#)]

44. Wang, S.; Zhou, N. Removal of carbamazepine from aqueous solution using sono-activated persulfate process. *Ultrason. Sonochem.* **2016**, *29*, 156–162. [[CrossRef](#)]
45. Li, Y.; Chen, Z.; Qi, J.; Kang, J.; Shen, J.; Yan, P.; Wang, W.; Bi, L.; Zhang, X.; Zhu, X. Degradation of bisphenol S by peroxymonosulfate activation through monodispersed CoFe_2O_4 nanoparticles anchored on natural palygorskite. *Sep. Purif. Technol.* **2021**, *277*, 119492. [[CrossRef](#)]
46. De Laat, J.; Le, G.T.; Legube, B. A comparative study of the effects of chloride, sulfate and nitrate ions on the rates of decomposition of H_2O_2 and organic compounds by $\text{Fe(II)/H}_2\text{O}_2$ and $\text{Fe(III)/H}_2\text{O}_2$. *Chemosphere* **2004**, *55*, 715–723. [[CrossRef](#)]
47. Li, J.; Xu, M.; Yao, G.; Lai, B. Enhancement of the degradation of atrazine through CoFe_2O_4 activated peroxymonosulfate (PMS) process: Kinetic, degradation intermediates, and toxicity evaluation. *Chem. Eng. J.* **2018**, *348*, 1012–1024. [[CrossRef](#)]
48. Li, J.; Yan, J.; Yao, G.; Zhang, Y.; Li, X.; Lai, B. Improving the degradation of atrazine in the three-dimensional (3D) electrochemical process using CuFe_2O_4 as both particle electrode and catalyst for persulfate activation. *Chem. Eng. J.* **2019**, *361*, 1317–1332. [[CrossRef](#)]
49. Liu, L.; Mi, H.; Zhang, M.; Sun, F.; Zhan, R.; Zhao, H.; He, S.; Zhou, L. Efficient moxifloxacin degradation by CoFe_2O_4 magnetic nanoparticles activated peroxymonosulfate: Kinetics, pathways and mechanisms. *Chem. Eng. J.* **2021**, *407*, 127201. [[CrossRef](#)]
50. Feng, Y.; Song, Q.; Lv, W.; Liu, G. Degradation of ketoprofen by sulfate radical-based advanced oxidation processes: Kinetics, mechanisms, and effects of natural water matrices. *Chemosphere* **2017**, *189*, 643–651. [[CrossRef](#)]
51. Giannakis, S.; Lin, K.-Y.A.; Ghanbari, F. A review of the recent advances on the treatment of industrial wastewaters by Sulfate Radical-based Advanced Oxidation Processes (SR-AOPs). *Chem. Eng. J.* **2021**, *406*, 127083. [[CrossRef](#)]
52. Gu, M.; Sui, Q.; Farooq, U.; Zhang, X.; Qiu, Z.; Lyu, S. Degradation of phenanthrene in sulfate radical based oxidative environment by nZVI-PDA functionalized rGO catalyst. *Chem. Eng. J.* **2018**, *354*, 541–552. [[CrossRef](#)]
53. Bian, X.; Xia, Y.; Zhan, T.; Wang, L.; Zhou, W.; Dai, Q.; Chen, J. Electrochemical removal of amoxicillin using a Cu doped PbO_2 electrode: Electrode characterization, operational parameters optimization and degradation mechanism. *Chemosphere* **2019**, *233*, 762–770. [[CrossRef](#)]
54. Wang, Y.; Shen, C.; Zhang, M.; Zhang, B.-T.; Yu, Y.-G. The electrochemical degradation of ciprofloxacin using a SnO_2 -Sb/Ti anode: Influencing factors, reaction pathways and energy demand. *Chem. Eng. J.* **2016**, *296*, 79–89. [[CrossRef](#)]
55. Hama Aziz, K.H.; Miessner, H.; Mueller, S.; Kalass, D.; Moeller, D.; Khorshid, I.; Rashid, M.A.M. Degradation of pharmaceutical diclofenac and ibuprofen in aqueous solution, a direct comparison of ozonation, photocatalysis, and non-thermal plasma. *Chem. Eng. J.* **2017**, *313*, 1033–1041. [[CrossRef](#)]
56. Shi, K.; Wang, Y.; Xu, A.; Zhou, X.; Zhu, H.; Wei, K.; Liu, X.; Shen, J.; Han, W. Efficient degradation of ibuprofen by electro-Fenton with microtubular gas-diffusion electrodes synthesized by wet-spinning method. *J. Electroanal. Chem.* **2021**, *897*, 115615. [[CrossRef](#)]
57. Wang, P.; Bu, L.; Wu, Y.; Ma, W.; Zhu, S.; Zhou, S. Mechanistic insight into the degradation of ibuprofen in UV/ H_2O_2 process via a combined experimental and DFT study. *Chemosphere* **2021**, *267*, 128883. [[CrossRef](#)]
58. Sun, S.; Hu, Y.; Xu, M.; Cheng, F.; Zhang, H.; Li, Z. Photo-Fenton degradation of carbamazepine and ibuprofen by iron-based metal-organic framework under alkaline condition. *J. Hazard. Mater.* **2022**, *424*, 127698. [[CrossRef](#)]
59. Liu, H.; Nkundabose, J.P.; Chen, H.; Yang, L.; Meng, C.; Ding, N. Decontamination of ibuprofen micropollutants from water based on visible-light-responsive hybrid photocatalyst. *J. Environ. Chem. Eng.* **2022**, *10*, 107154. [[CrossRef](#)]
60. Li, C.; Lin, H.; Armutlulu, A.; Xie, R.; Zhang, Y.; Meng, X. Hydroxylamine-assisted catalytic degradation of ciprofloxacin in ferrate/persulfate system. *Chem. Eng. J.* **2019**, *360*, 612–620. [[CrossRef](#)]
61. Tsitonaki, A.; Petri, B.; Crimi, M.; Mosbæk, H.; Siegrist, R.; Bjerg, P. In Situ Chemical Oxidation of Contaminated Soil and Groundwater Using Persulfate: A Review. *Crit. Rev. Environ. Sci. Technol.* **2010**, *40*, 55–91. [[CrossRef](#)]
62. Jaafarzadeh, N.; Ghanbari, F.; Zahedi, A. Coupling electrooxidation and Oxone for degradation of 2,4-Dichlorophenoxyacetic acid (2,4-D) from aqueous solutions. *J. Water Process Eng.* **2018**, *22*, 203–209. [[CrossRef](#)]
63. Jin, Y.; Sun, S.-P.; Yang, X.; Chen, X.D. Degradation of ibuprofen in water by FeII-NTA complex-activated persulfate with hydroxylamine at neutral pH. *Chem. Eng. J.* **2018**, *337*, 152–160. [[CrossRef](#)]
64. Liu, S.-H.; Tang, W.-T.; Chou, P.-H. Microwave-assisted synthesis of triple 2D $\text{g-C}_3\text{N}_4/\text{Bi}_2\text{WO}_6/\text{rGO}$ composites for ibuprofen photodegradation: Kinetics, mechanism and toxicity evaluation of degradation products. *Chem. Eng. J.* **2020**, *387*, 124098. [[CrossRef](#)]
65. Ma, M.; Chen, L.; Zhao, J.; Liu, W.; Ji, H. Efficient activation of peroxymonosulfate by hollow cobalt hydroxide for degradation of ibuprofen and theoretical study. *Chin. Chem. Lett.* **2019**, *30*, 2191–2195. [[CrossRef](#)]
66. Marković, M.; Jović, M.; Stanković, D.; Kovačević, V.; Roglič, G.; Gojgić-Cvijović, G.; Manojlović, D. Application of non-thermal plasma reactor and Fenton reaction for degradation of ibuprofen. *Sci. Total Environ.* **2015**, *505*, 1148–1155. [[CrossRef](#)] [[PubMed](#)]
67. Yadav, A.A.; Hunge, Y.M.; Kulkarni, S.B. Synthesis of multifunctional FeCo_2O_4 electrode using ultrasonic treatment for photocatalysis and energy storage applications. *Ultrason. Sonochem.* **2019**, *58*, 104663. [[CrossRef](#)]